Science
AAAS

Glia Promote Local Synaptogenesis Through UNC-6 (Netrin) Signaling in C. elegans
Daniel A. Colón-Ramos, *et al.*
Science **318**, 103 (2007);
DOI: 10.1126/science.1143762

2. P. J. S. Olney, G. M. Mace, A. Feistner, *Creative Conservation: Interactive Management of Wild and Captive Animals* (Chapman & Hall, London, ed. 1, 1994).
3. R. Frankham, D. A. Briscoe, J. D. Ballou, *Introduction to Conservation Genetics* (Cambridge Univ. Press, Cambridge, 2002).
4. M. Lynch, M. O' Hely, *Conserv. Genet.* **2**, 363 (2001).
5. M. J. Ford, *Conserv. Biol.* **16**, 815 (2002).
6. D. Goodman, *Can. J. Fish. Aquat. Sci.* **62**, 374 (2005).
7. W. R. Heard, "An estimate of total 1992 hatchery releases of the North Pacific Ocean and adjacent seas." [North Pacific Anadromous Fish Commission Doc. 154, Auke Bay Fisheries Laboratory, Alaska Fisheries Science Center, National Marine Fisheries Service (NMFS), National Oceanic and Atmospheric Administration (NOAA), Juneau, AK, 1995].
8. X. Augerot, D. N. Foley, *Atlas of Pacific Salmon: The First Map-Based Status Assessment of Salmon in the North Pacific* (Univ. of California Press, Berkeley, CA, 2005).
9. R. N. Williams, *Return to the River: Restoring Salmon to the Columbia River* (Elsevier Academic Press, Amsterdam, 2006).
10. I. A. Fleming *et al.*, *Proc. R. Soc. London Ser. B* **267**, 1517 (2000).
11. I. A. Fleming, E. Peterson, *Nord. J. Freshw. Res.* **75**, 71 (2001).
12. B. Berejikian, M. J. Ford, "Review of relative fitness of hatchery and natural salmon." (NMFS-NWFSC-61, Northwest Fisheries Science Center, Seattle, WA, 2004).
13. R. R. Reisenbichler, J. D. McIntyre, *Can. J. Fish. Res. Board* **34**, 123 (1977).
14. D. D. Heath, J. W. Heath, C. A. Bryden, R. M. Johnson, C. W. Fox, *Science* **299**, 1738 (2003).
15. T. N. Pearsons, A. L. Fritts, J. L. Scott, *Can. J. Fish. Aquat. Sci.* **64**, 803 (2007).
16. A. L. Fritts, J. L. Scott, T. N. Pearsons, *Can. J. Fish. Aquat. Sci.* **64**, 813 (2007).
17. H. Araki, W. R. Ardren, E. Olsen, B. Cooper, M. S. Blouin, *Conserv. Biol.* **21**, 181 (2007).
18. B. A. Berejikian, E. P. Tezak, S. L. Schroder, C. M. Knudsen, J. J. Hard, *ICES J. Mar. Sci.* **54**, 1040 (1997).
19. Methods are available as supporting material on *Science* Online.
20. H. Araki, M. S. Blouin, *Mol. Ecol.* **14**, 4097 (2005).
21. M. J. Hercus, A. A. Hoffmann, *Proc. R. Soc. London Ser. B* **267**, 2105 (2000).
22. A. Kyneb, S. Toft, *Ecol. Entomol.* **31**, 322 (2006).
23. D. Reznick, *Evolution Int. J. Org. Evolution* **35**, 941 (1981).
24. J. Lindström, *Trends Ecol. Evol.* **14**, 343 (1999).
25. "Report for the meeting held August 20 to September 2, 2004" (Salmon Recovery Science Review Panel, Northwest Fisheries Science Center, Seattle, 2004).
26. We thank R. S. Waples, M. Ford, and four anonymous reviewers for helpful discussions, W. R. Ardren, C. Criscione, R. VanDam and the Center for Genome Research and Biocomputing in Oregon State University for help with laboratory work and E. Olsen, R. French, J. Gidley, and staff of the Oregon Department of Fish and Wildlife (ODFW) for technical help and advice. This research was funded by contracts to M.S.B. from the Bonneville Power Administration and the ODFW.

Glia Promote Local Synaptogenesis Through UNC-6 (Netrin) Signaling in *C. elegans*

Daniel A. Colón-Ramos,[1] Milica A. Margeta,[1,2] Kang Shen[1,2]*

Neural circuits are assembled through the coordinated innervation of pre- and postsynaptic partners. We show that connectivity between two interneurons, AIY and RIA, in *Caenorhabditis elegans* is orchestrated by a pair of glial cells that express UNC-6 (netrin). In the postsynaptic neuron RIA, the netrin receptor UNC-40 (DCC, deleted in colorectal cancer) plays a conventional guidance role, directing outgrowth of the RIA process ventrally toward the glia. In the presynaptic neuron AIY, UNC-40 (DCC) plays an unexpected and previously uncharacterized role: It cell-autonomously promotes assembly of presynaptic terminals in the immediate vicinity of the glial cell endfeet. These results indicate that netrin can be used both for guidance and local synaptogenesis and suggest that glial cells can function as guideposts during the assembly of neural circuits in vivo.

Neural circuit formation requires an intricate orchestration of multiple developmental events, including cell migration, axon guidance, dendritic growth, synaptic target selection, and synaptogenesis (*1–3*). These developmental events are coordinated in pre- and postsynaptic neuronal partners to form the functional neural circuits that underlie behaviors. Although the organization and specificity of these neural circuits is well documented, the cellular and molecular mechanisms that underlie their precise development are not well understood.

To explore how precise neural connectivity is achieved, we studied the synaptic connections between two interneurons in the *C. elegans* brain: presynaptic AIY and postsynaptic RIA. These two interneurons navigate complex cellular environments, discriminating among multiple potential targets before finding and innervating each other at a discrete region of their respective processes (*4*). We generated single-cell fluorescent markers to visualize AIY-RIA connectivity in vivo and observed a discrete clustering of presynaptic AIY markers in a segment of the process we termed zone 2. This zone appears to be the specialized presynaptic region where AIY forms synapses onto RIA, as well as RIB and AIZ neurons. First, the fluorescently labeled presynaptic proteins RAB-3, ELKS-1, and SYD-2 are all more concentrated in zone 2 than in other regions of the axon (Figs. 1A and 2B and fig. S4A). Second, these markers cluster at the exact location at which AIY to RIA synapses are seen in electron micrographs of wild-type animals (fig. S1M) (*5*). Third, this region has a wider diameter than other regions of the axon, a property that we found to be uniquely associated with the presynaptic region of AIY in electron micrographs (fig. S1, A and M to Q). These combined properties were taken as evidence of presynaptic differentiation and were very reproducible across animals (Fig. 1 and fig. S1).

Reconstructions of electron microscopy (EM) micrographs (*5*) revealed that AIY has three distinct anatomical regions throughout its process: a segment proximal to the AIY cell body that is devoid of synapses (zone 1); the synapse-rich region where AIY forms synapses onto RIA, AIZ, and RIB just as the AIY process turns dorsally (zone 2); and a distal axon segment within the nerve ring that has four to eight small presynaptic specializations (zone 3).

To identify the molecular signals that direct this precise innervation, we performed a visual genetic screen for mutants with an abnormal synapse distribution in AIY. From this screen, we isolated the *wy81* mutation, an allele of *unc-40* (fig. S2). UNC-40 (DCC, deleted in colorectal cancer) is a transmembrane immunoglobulin superfamily protein that is a receptor for the axon guidance molecule UNC-6 (netrin) (*6*, *7*). *unc-40* animals had no detectable axon guidance defects in AIY except for an axon truncation defect observed in 7.8% of the animals ($n = 153$ animals; fig. S3). However, they showed a highly penetrant defect in the presynaptic specialization of AIY at zone 2: 95.3% of *unc-40(wy81)* animals displayed a severe reduction of active zone markers ELKS-1::YFP (yellow fluorescent protein) and SYD-2::GFP (green fluorescent protein) and a synaptic vesicle marker, mCherry::RAB-3, in zone 2 ($n = 128$ animals; Fig. 2, A to K, and fig. S4). In addition, the AIY axon diameter in zone 2 failed to widen into the characteristic presynaptic varicosity seen in wild-type animals (fig. S1). By contrast, in the more-dorsal zone 3 synaptic regions, *unc-40* animals had normal or increased levels of synaptic vesicle proteins and a normal or increased diameter (Fig. 2, F to I, and fig. S1). These defects suggest a specific defect in the presynaptic differentiation of AIY in zone 2, although a detailed analysis of AIY synaptic ultrastructure and function could

[1]Department of Biological Sciences, Stanford University, 144 Herrin Laboratories, Stanford, CA 94305–5020, USA. [2]Neurosciences Program, Stanford University, Stanford, CA 94305–5020, USA.

*To whom correspondence should be addressed. E-mail: kangshen@stanford.edu

reveal abnormalities in other AIY synapses. Although *unc-40* animals do not have substantial AIY axon guidance defects, RIA axon guidance is severely affected in *unc-40* mutants: RIA processes fail to extend ventrally to create the loop that is innervated by AIY in zone 2 (95.8% penetrant, $n = 191$ animals; fig. S3).

To identify the cell(s) in which *unc-40* functions to direct AIY-RIA innervation, we analyzed *unc-40* mosaic animals that retain an unstable rescuing array in subsets of cells (*8*). Interestingly, only when the array was retained in the AIY interneuron did we observe significant rescue of the AIY presynaptic patterning defects ($P < 0.001$; Fig. 2, L to M, and figs. S5 and S6). Retention of the array in the closely related interneuron RIB or RIM (RIB/RIM) (*9*) did not result in rescue. Retention in the RIA interneuron resulted in rescue of the RIA axon guidance defect but not of the AIY presynaptic phenotype (fig. S7).

Together, these data indicate that axon guidance of RIA and patterning of presynaptic specializations in AIY are independent, cell-autonomous events. These mosaic analyses are also consistent with the observation that UNC-40 (DCC) is endogenously expressed in AIY interneurons (fig. S6) and indicate a previously uncharacterized role for UNC-40 (DCC) in specifying AIY presynaptic terminals in a cell-autonomous manner.

To determine how UNC-40 (DCC) directs presynaptic assembly in AIY, we examined its subcellular localization. Consistent with UNC-40 (DCC) playing a role in the presynaptic patterning of AIY, we observed that UNC-40 (DCC) is enriched in zones 2 and 3, the regions where

presynaptic sites are assembled (Fig. 3, A and C; 71.5% animals with enriched localization, $n = 214$ animals). This enrichment is dependent on UNC-6 (netrin), because UNC-40 (DCC) failed to concentrate at the presynaptic sites of AIY in *unc-6* animals (Fig. 3, B and C; 87.6% with diffuse localization, $n = 201$ animals). Consistent with this observation, in *unc-6* animals circuit assembly between AIY and RIA is abnormal, phenocopying the *unc-40* mutant defect (fig. S8).

During neurulation, when AIY-RIA innervation takes place, UNC-6 (netrin) is exclusively expressed by ventral cephalic sheath cells (VCSCs) at the nerve ring (*10*). VCSCs are non-neuronal cells that are morphologically similar to vertebrate astrocytes (*11*). Mosaic analysis using an *unc-6* rescuing construct showed that expression of UNC-6 (netrin) by VCSCs regulates the pattern of AIY presynapses (fig. S8B, $P < 0.001$).

VCSCs have slender processes that enter the nerve ring and terminate at specific synaptic sites, one of them being zone 2, the region where AIY innervates RIA (*4*). We investigated the physical relations between the VCSCs, AIY, and RIA and observed that the VCSCs project endfeet to the anterior end of the ventral nerve cord and form deeply invaginated membrane lamellae that ensheath the zone 2 region where AIY innervates RIA. The relative positioning of the VCSC endfeet with respect to AIY and RIA is extremely stereotyped across animals, revealing a tight and reproducible anatomical relation between the UNC-6–secreting VCSCs and the AIY-RIA synapses (Fig. 3, D to J, and fig. S1).

To test further whether the precise anatomical relation between the sheath cells and AIY-RIA synapses is instructive in mediating AIY:RIA in-
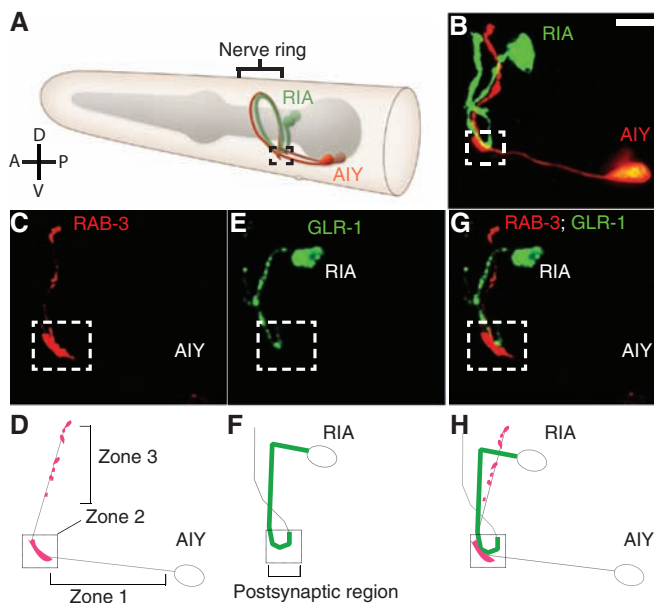
nervation, we identified mutants that disrupt sheath cell morphology. We found that mutations in *unc-34*/enabled, a regulator of the actin cytoskeleton, altered the morphology of cephalic sheath cells: 47.8% of the *unc-34* animals have distended endfeet, which project further posteriorly ($n = 94$ animals; Fig. 4, A and D, and fig. S9A). In these *unc-34* animals, the distended VCSCs ectopically ensheath zone 1 of AIY in addition to zones 2 and 3 (Fig. 4, A and D). Also in these animals, we observed a change in the distribution of UNC-40 (DCC), which ectopically localized to zone 1 (Fig. 4, E to G). Furthermore, there was a concomitant change in the distribution of AIY presynapses: ectopic AIY presynaptic specializations now formed in zone 1, the region of overlap with distended sheath cell endfeet where ectopic UNC-40 localized (Fig. 4, B and D). Moreover, RIA axon guidance changed accordingly, with the RIA postsynaptic loop extending further posteriorly to the region covered by the sheath cell endfeet ($P < 0.001$; Fig. 4, C and D, and fig. S9A).

An epistasis analysis confirmed that the displacement of presynaptic sites observed in *unc-34* animals is an UNC-40 (DCC)–dependent event (fig. S9, B to D). These observations are consistent with a model whereby UNC-34 (enabled) affects presynaptic patterning in AIY by altering sheath cell morphology, which then affects localized UNC-6 (netrin) secretion, UNC-40 (DCC) localization, and presynaptic assembly.

Together our data strongly suggest that glia act as guideposts in directing circuit assembly between AIY and RIA. The glial cells mark a neurospatial coordinate in the *C. elegans* nerve ring through the secretion of UNC-6 (netrin). This in turn signals to AIY and RIA neurons through UNC-40 (DCC). UNC-40 (DCC) simultaneously activates two different and independent pathways in each neuron, orchestrating presynaptic assembly in AIY and axon guidance of postsynaptic RIA to the glial-specified location.

How can the same receptor and ligand elicit diverse cellular responses in distinct neurons? UNC-40 (DCC) has been reported to regulate diverse developmental processes like cell migration, neuronal polarization, and axon guidance, all of which involve an initial polarization event that may be mediated by netrin signaling (*6, 7, 12–15*). The patterning of AIY presynaptic regions can also be considered a local polarization event, through which AIY transforms a region of its plasma membrane into a specialized presynaptic area. Other guidance molecules, such as the Eph family of receptors and their ephrin ligands, have been shown to play roles in growth cone guidance as well as the development of mature excitatory synapses (*16*). In ephrin-mediated signaling, distinct cellular responses are likely generated by the developmental context and by diverse downstream targets (*17*). Similar mechanisms could explain the distinct cellular responses to UNC-40 (DCC) signaling.

Fig. 1. AIY and RIA innervate at a specific spatial coordinate in the nerve ring. (**A**) Schematic diagram of the morphology of the presynaptic AIY and postsynaptic RIA neurons in the nerve ring (brackets). Modified image adapted from www.wormatlas.org with permission. (**B**) Representative adult animal expressing cytoplasmic fluorophores specifically in AIY (red) and RIA (green). In all images, the dashed box (zone 2 in text) delineates a spatial coordinate in the wild-type nerve ring where the RIA and the AIY interneurons converge and synapse onto each other. (**C** to **H**) Confocal micrographs and corresponding diagrams demonstrating the colocalization of AIY presynaptic vesicles [CFP::RAB-3 and pseudocolored red in (C)] with postsynaptic RIA glutamate receptors [GLR-1::YFP and pseudocolored green in (E)] in zone 2 (dashed box). Double labels are shown in (G). Schematic diagrams [(D), (F), and (H)] show the relation between AIY presynaptic terminals and the RIA postsynaptic region, which was highly reproducible across animals ($n > 500$). Scale bars, 5 μm.

Fig. 2. UNC-40 (DCC) is required for correct presynaptic patterning in AIY. (**A** to **J**) Distribution of presynaptic sites of AIY in wild-type [(A) to (E)] or *unc-40* [(F) to (J)] animals. Confocal micrographs demonstrate the colocalization and patterning of AIY presynaptic vesicles [mCherry::RAB-3 pseudocolored red in (A) and (F)] and active zones [ELKS-1/ERC::YFP pseudocolored green in (B) and (G)] in a representative wild-type [(A) to (C)] or *unc-40* [(F) to (H)] animal, evident in the double-label merge images [(C) and (H)] and represented in the diagram of presynaptic site distribution [(D) and (I)]. Three-dimension line scan profiles of the fluorescence intensity (arbitrary units, AU) distribution in (A) and (F). (**K**) Quantification comparing the relative distribution of synaptic vesicle fluorescence in wild-type (blue; $n = 20$ neurons) versus *unc-40* animals (red; $n = 31$ neurons). Error bars represent standard error, and the asterisk represents statistical significance ($P < 0.001$). (**L** and **M**) *unc-40* (e271) animals expressing an unstable transgene containing an *unc-40* rescuing construct, and cytoplasmic cell-specific markers in AIY and RIA (L) or RIB/RIM (M) were scored for retention of the transgene and rescue of the AIY presynaptic phenotype. ***$P < 0.001$, **$P < 0.01$, and *$P < 0.05$ between indicated groups. Scale bars, 5 μm.
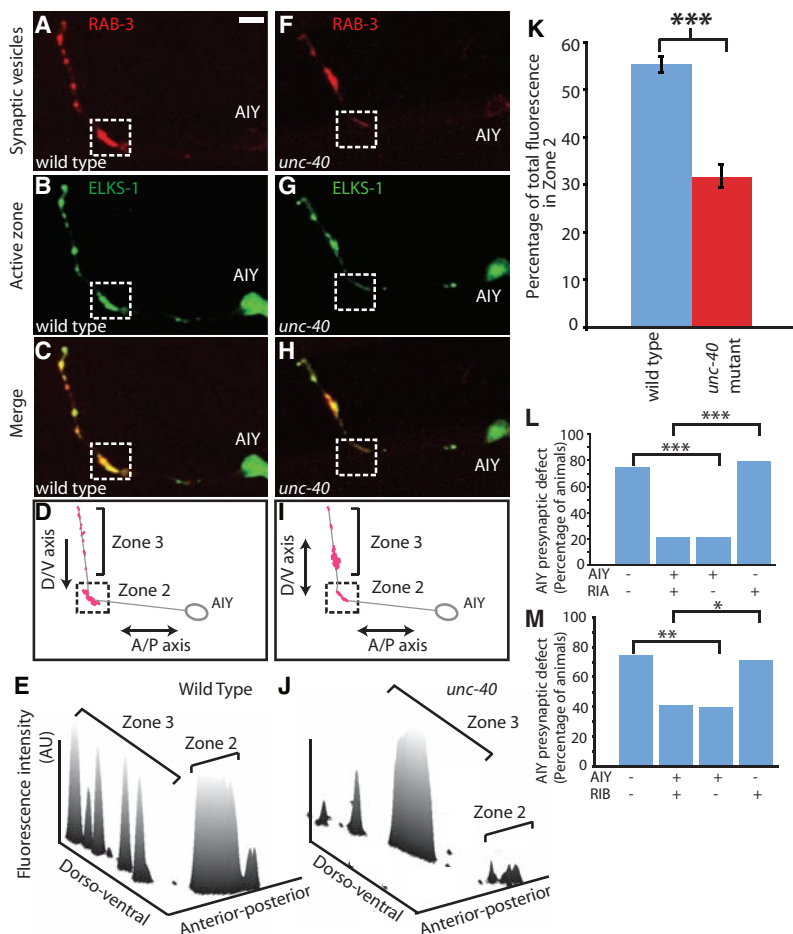

Fig. 3. Ventral cephalic sheath cells control UNC-40 (DCC) enrichment in presynaptic regions by secreting UNC-6 (netrin). (**A** and **B**) Localization of UNC-40::GFP in AIY of a representative wild-type (A) or *unc-6* (B) animal. Note UNC-40:GFP enrichment in zones 2 and 3 in wild-type animals [(A) dashed box], as compared to diffuse localization in *unc-6* animals (B). (**C**) Quantification of the enrichment of UNC-40::GFP in the presynaptic regions of wild-type versus *unc-6* animals. Two different transgenic lines (lines 1 or 2), both expressing UNC-40::GFP, were scored. (**D**) Projection of confocal micrographs obtained from a representative animal simultaneously expressing *hlh-17::mCherry* (to label ventral cephalic sheath cells and pseudocolored blue), *ttx-3::cfp::rab-3* (to label presynapses in AIY and pseudocolored red), and *glr-3::glr-1::yfp* (to label the glutamate receptors in RIA and pseudocolored green). (**E**) Volume rendering of (D) showing the relative positioning of the glial-like ventral cephalic sheath cells with respect to the region of innervation between AIY and RIA (29). (**F**) Diagram of (D) and (E). The asterisk marks the posterior extension of the sheath cell. (**G**) Volume rendering of the ventral sheath cell in (D). Note the groove in the boxed region where AIY and RIA are ensheathed by the ventral cephalic sheath cells and innervate each other. (**H** and **I**) Single confocal plane of (D), with presynaptic vesicles in AIY [labeled with cyan fluorescent protein (CFP)::RAB-3 and pseudocolored red in (H)], glutamate receptors in RIA [labeled with GLR-1:YFP and pseudocolored green in (I)] and a triple label including expression of the mCherry cytoplasmic fluorophore in the sheath cells [pseudocolored blue in (J)]. This anatomical relation was extremely stereotyped across animals ($n > 500$). Scale bars, 5 μm.
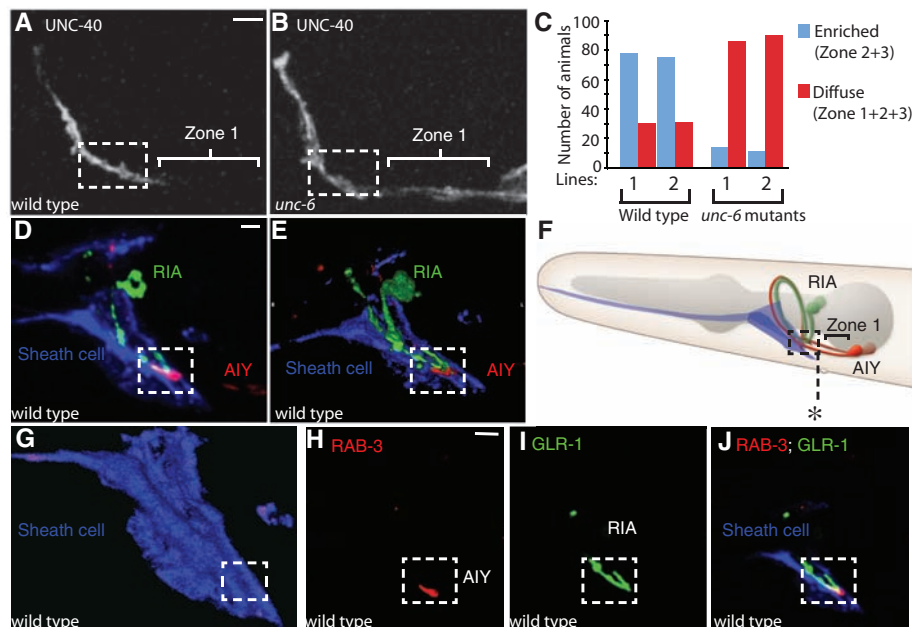
Fig. 4. Repositioning of the sheath cells affects RIA axon guidance and AIY presynapses. (**A**) Diagram showing the distended positioning of the ventral cephalic sheath cell in *unc-34* animals. The asterisk marks the normal posterior boundary of a wild-type sheath cell (see Fig. 3F for comparison). In *unc-34*, animals sheath cells abnormally distend posteriorly in 47.9% of animals (*n* = 94 animals). (**B** to **D**) Confocal micrographs obtained from a representative *unc-34* animal simultaneously expressing *ttx-3::cfp::rab-3* [to label presynapses in AIY and pseudocolored red in (B) and (D)], *glr-3::glr-1::yfp* [to label the glutamate receptors in RIA and pseudocolored green in (C) and (D)], and *hlh-17::mCherry* [to label the ventral cephalic sheath cells and pseudocolored blue in (D)]. Note abnormal posterior extension of the sheath cell endfeet, corresponding ectopic AIY presynapses in zone 1, and distended RIA axon in the area now covered by the distended sheath cell (compare with Fig. 3D). (**E** to **G**) Confocal micrographs obtained from a representative *unc-34* animal simultaneously expressing *ttx-3::mCherry::rab-3* [to label presynapses in AIY and pseudocolored red in (E) and (G)] and *ttx-3::unc-40::gfp* [to label the UNC-40 (DCC) receptors in AIY and pseudocolored green in (F) and (G)]. Scale bars, 5 μm.
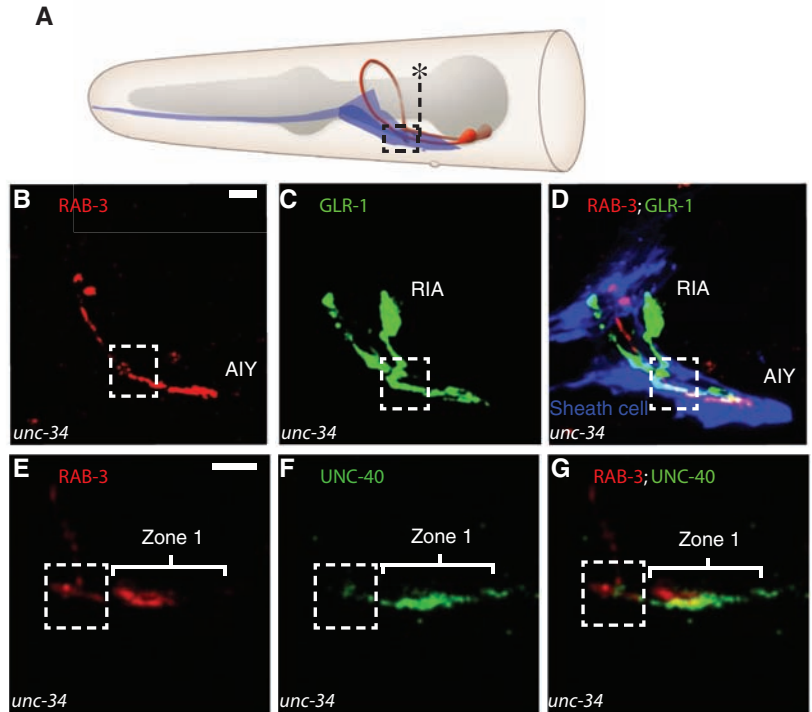
Although cell-specific events in AIY and RIA happen independently of each other, their simultaneous regulation by a single molecule allows coordinated circuit assembly. UNC-6 (netrin) is a secreted chemotropic factor that can act as a long-range chemical cue or a short-range signaling molecule, depending on the developmental context (*18–20*). Given the close anatomical relation between the source of UNC-6 (netrin) (VCSCs) and the AIY:RIA synapses, it is likely that UNC-6 (netrin) acts as a short-range signaling molecule in this pathway, specifying microenvironments that promote UNC-40 (DCC) enrichment and synaptogenesis. Indeed, vertebrate astrocytes have been shown to be functionally compartmentalized into subcellular microdomains, which may be important in regulating localized secretion of signaling molecules regulating synaptic assembly and function (*21*). Furthermore, UNC-6 (netrin) has been reported to mediate adhesive interactions and function as a short-range target recognition molecule in other developmental events (*18, 19, 22*).

Our study is consistent with observations made in vertebrates and highlights the importance of glial cells in specifying precise neural connectivity. The fact that dissociated cultured neurons can form functional synapses in the absence of glial cells suggests that pre- and postsynaptic neurons are sufficient to assemble chemical synapses. However, growing evidence suggests that glia are essential regulators of synaptic assembly and function in vivo (*11, 23–26*). For instance, astrocyte-secreted thrombospondin increases the density of synapses in the mammalian central nervous system (*23, 27*).

Our data show that glia can also specify neural connectivity in vivo by marking a neuro-spatial coordinate, which achieves precise circuit assembly by controlling both synaptic partner choices and the location of innervation. Such stereotyped synaptic assembly gives rise to highly organized neuropil structures such as the nematode nerve ring. Similarly organized neuropil structures are also evident throughout the vertebrate central nervous system, exemplified by the stratified organization of the inner plexiform layer of the vertebrate retina and the glomeruli in the olfactory bulb (*2, 28*). The roles observed here for glia in *C. elegans* may be evolutionarily conserved, such that proteins with multifunctional roles in spatial patterning, like UNC-40 (DCC), would detect the localized expression of glial signals and thus orchestrate the formation of neural circuits.

References and Notes

1. R. Salie, V. Niederkofler, S. Arber, *Neuron* **45**, 189 (2005).
2. R. Juttner, F. G. Rathjen, *Cell. Mol. Life Sci.* **62**, 2811 (2005).
3. C. L. Waites, A. M. Craig, C. C. Garner, *Annu. Rev. Neurosci.* **28**, 251 (2005).
4. J. G. White, E. Southgate, J. N. Thomson, S. Brenner, *Philos. Trans. R. Soc. London Ser. B* **314**, 1 (1986).
5. J. G. White, E. Southgate, J. N. Thomson, S. Brenner, *Cold Spring Harbor Symp. Quant. Biol.* **48**, 633 (1983).
6. S. S. Chan *et al.*, *Cell* **87**, 187 (1996).
7. K. Keino-Masu *et al.*, *Cell* **87**, 175 (1996).
8. J. Yochem, R. K. Herman, *Development* **130**, 4761 (2003).
9. Materials and methods are available on *Science* Online.
10. W. G. Wadsworth, H. Bhatt, E. M. Hedgecock, *Neuron* **16**, 35 (1996).
11. S. Shaham, *Curr. Opin. Neurobiol.* **16**, 522 (2006).
12. C. E. Adler, R. D. Fetter, C. I. Bargmann, *Nat. Neurosci.* **9**, 511 (2006).
13. E. M. Hedgecock, J. G. Culotti, D. H. Hall, *Neuron* **4**, 61 (1990).
14. E. D. Leonardo *et al.*, *Cold Spring Harbor Symp. Quant. Biol.* **62**, 467 (1997).
15. E. Bloch-Gallego, F. Ezan, M. Tessier-Lavigne, C. Sotelo, *J. Neurosci.* **19**, 4407 (1999).
16. M. B. Dalva *et al.*, *Cell* **103**, 945 (2000).
17. K. K. Murai, E. B. Pasquale, *Neuroscientist* **10**, 304 (2004).
18. K. A. Baker, S. W. Moore, A. A. Jarjour, T. E. Kennedy, *Curr. Opin. Neurobiol.* **16**, 529 (2006).
19. P. Strickland, G. C. Shin, A. Plump, M. Tessier-Lavigne, L. Hinck, *Development* **133**, 823 (2006).
20. M. Brankatschk, B. J. Dickson, *Nat. Neurosci.* **9**, 188 (2006).
21. P. G. Haydon, G. Carmignoto, *Physiol. Rev.* **86**, 1009 (2006).
22. M. L. Winberg, K. J. Mitchell, C. S. Goodman, *Cell* **93**, 581 (1998).
23. N. J. Allen, B. A. Barres, *Curr. Opin. Neurobiol.* **15**, 542 (2005).
24. M. R. Freeman, *Curr. Opin. Neurobiol.* **16**, 119 (2006).
25. P. Jourdain *et al.*, *Nat. Neurosci.* **10**, 331 (2007).
26. H. Nishida, S. Okabe, *J. Neurosci.* **27**, 331 (2007).
27. K. S. Christopherson *et al.*, *Cell* **120**, 421 (2005).
28. T. Komiyama, L. Luo, *Curr. Opin. Neurobiol.* **16**, 67 (2006).
29. We thank G. Wang, C. Johnson, J. Audhya, M. Nonet, Y. Kohara, J. Kaplan, G. Garriga, E. Lundquist, the *Caenorhabditis* Genetic Center, and the Japanese National BioResource Project for strains and reagents; D. Hall and Z. Altun for diagrams used in the figures; C. Bargmann for helpful discussions and generous sharing of advice and reagents; C. Gao and Frank Chen for technical assistance; and S. Margolis, L. Looger, J. Irazoqui, B. Barres, and members of the Shen lab for thoughtful comments on the manuscript. This work was funded by grants to K.S. from the following: the McKnight Endowment Fund, the W. M. Keck Foundation, and the Searle Scholar program. M.A.M. was supported by the Stanford Medical Scientist Training Program and NIH grant GM007365. D.A.C.-R. was supported by the Damon Runyon Foundation and NIH grant K99 NS057931-01.